



HAL
open science

A pseudo-spectral method with volume penalisation for magnetohydrodynamic turbulence in confined domains

Kai Schneider, Salah Neffaa, Wouter J.T. Bos

► **To cite this version:**

Kai Schneider, Salah Neffaa, Wouter J.T. Bos. A pseudo-spectral method with volume penalisation for magnetohydrodynamic turbulence in confined domains. *Computer Physics Communications*, 2011, 182 (1), pp.2-7. 10.1016/j.cpc.2010.05.019 . hal-00647827

HAL Id: hal-00647827

<https://hal.science/hal-00647827>

Submitted on 17 Aug 2022

HAL is a multi-disciplinary open access archive for the deposit and dissemination of scientific research documents, whether they are published or not. The documents may come from teaching and research institutions in France or abroad, or from public or private research centers.

L'archive ouverte pluridisciplinaire **HAL**, est destinée au dépôt et à la diffusion de documents scientifiques de niveau recherche, publiés ou non, émanant des établissements d'enseignement et de recherche français ou étrangers, des laboratoires publics ou privés.



Distributed under a Creative Commons Attribution - NonCommercial 4.0 International License

A pseudo-spectral method with volume penalisation for magnetohydrodynamic turbulence in confined domains

Kai Schneider^{a,*}, Salah Neffaa^a, Wouter J.T. Bos^b

^a M2P2–CNRS & CMI, Aix-Marseille University, Marseille, France

^b LMFA–CNRS, Ecole Centrale de Lyon – Université de Lyon, Ecully, France

We present a Fourier pseudo-spectral method for solving the resistive magnetohydrodynamic equations of incompressible flow in confined domains. A volume penalisation method allows to take into account boundary conditions and the geometry of the domain. A code validation is presented for the z-pinch test case. Numerical simulations of decaying MHD turbulence in two space dimensions show spontaneous spin-up of the flow in non-axisymmetric geometries, which is reflected by the generation of angular momentum. First results of decaying MHD turbulence in a cylinder illustrate the potential of the new method for three-dimensional simulations.

1. Introduction

In magnetohydrodynamic (MHD) as in hydrodynamic turbulence (HD), the main challenge in direct numerical simulation (DNS) is to take into account boundary conditions imposed by the physics of the problem without compromising the stability and precision of the numerical scheme. For homogeneous turbulence, either HD or MHD, for which periodic boundary conditions can be used, pseudo-spectral methods using Fast Fourier transforms are still the most precise and efficient schemes [8,12] which are now available since many decades. However, non-periodic boundary conditions and complexly shaped geometries require more advanced numerical schemes. Spectral methods become more complicated for nonperiodic boundary conditions, because of the use of, e.g., Tchebycheff or Bessel functions and they are still limited to simple geometries.

Boundary conditions in confined HD turbulence are typically of no-slip or of slip type. In MHD turbulence the situation is more delicate as the boundary conditions for the magnetic field depend on the surrounding domain of the electrically conducting fluid. In the case of a perfect conductor the magnetic field simply vanishes outside, however special care has to be taken for the current density. One physically motivated type of boundary conditions consists in supposing that the perfect conductor is coated inside with a thin layer of insulant, such that the current density cannot pen-

trate into the solid [13]. In the case of surrounding vacuum the magnetic field has to be prolonged outside the fluid domain and matched with the magnetic field in the fluid region [15].

An efficient method to compute HD flows in the presence of solid obstacles and walls is the volume penalisation approach which was introduced by Angot et al. [1] for the Navier–Stokes equations and applied to hydrodynamic turbulence in [16,17]. This method was extended to MHD turbulence in a recent work [2,14]. Using this method, efficient pseudo-spectral solvers can be used to compute flows which contain solid walls and obstacles, which may even move in time [10].

In the present paper we describe the volume penalisation method in combination with a pseudospectral method for resistive MHD equations of incompressible flow in confined domains. The governing equations are modified by adding penalisation terms which contain a mask function which describes the geometry of the domain. The therewith imposed boundary conditions are vanishing velocity and no penetration of magnetic field into the solid domain which is hence considered as a perfect conductor, coated inside with a thin layer of insulant, which guarantees that the current density cannot penetrate into the solid. The governing penalised MHD equations and their numerical space and time discretization are presented in a concise way. Therewith we perform pseudo-spectral simulations of 2D MHD flows in bounded domains. A code validation is presented together with a convergence study for the z-pinch. Then we investigate decaying 2D MHD turbulence in two different confined domains and show that spontaneous spin-up takes place in the considered non-axisymmetric geometries. This phenomenon, observed in [2] at low Reynolds number (Re), persists at higher Re and becomes more pronounced.

* Corresponding author.

E-mail address: kscheid@cmi.univ-mrs.fr (K. Schneider).

URL: <http://www.cmi.univ-mrs.fr/~kscheid> (K. Schneider).

We also show some preliminary computations of 3D decaying MHD turbulence in a cylinder, which illustrates the potential of the new method for three-dimensional MHD.

The remainder of the paper is organized as follows. In the following section the governing equations are presented together with the volume penalisation to impose the boundary conditions. In Section 3 the numerical method, a pseudospectral method with semi-implicit time discretization is exposed. Section 4 presents a couple of numerical results in two and three space dimensions to illustrate the numerical scheme. Finally, conclusions are drawn in Section 5.

2. MHD meets volume penalisation

The velocity field \mathbf{u} and the magnetic field \mathbf{B} of an electrically conducting incompressible fluid in a domain Ω_f are governed by the following dimensionless equations,

$$\frac{\partial \mathbf{u}}{\partial t} + \mathbf{u} \cdot \nabla \mathbf{u} = -\nabla p + \mathbf{j} \times \mathbf{B} + \nu \nabla^2 \mathbf{u} - \frac{1}{\epsilon} \chi (\mathbf{u} - \mathbf{u}_0) \quad (1)$$

$$\frac{\partial \mathbf{B}}{\partial t} = \nabla \times (\mathbf{u} \times \mathbf{B}) + \eta \nabla^2 \mathbf{B} - \frac{1}{\epsilon} \chi (\mathbf{B} - \mathbf{B}_0) \quad (2)$$

$$\nabla \cdot \mathbf{u} = \nabla \cdot \mathbf{B} = 0 \quad (3)$$

where ν is the kinematic viscosity, η the magnetic diffusivity, p the pressure and $\mathbf{j} = \nabla \times \mathbf{B}$ the current density. The above equations are considered in a computational domain $\Omega = \Omega_f \cup \Omega_s$ in which the fluid domain Ω_f is embedded. The solid domain Ω_s encloses Ω_f and the mask function $\chi(\mathbf{x})$ entirely determines the geometry of the domain.

The mask function is given by

$$\chi_{\Omega_s}(\mathbf{x}) = \begin{cases} 1 & \text{for } \mathbf{x} \in \bar{\Omega}_s \\ 0 & \text{elsewhere} \end{cases} \quad (4)$$

The last term in the evolution equations for \mathbf{u} and \mathbf{B} , is the penalisation term which allows to impose the solid boundary conditions. Thus both the fluid-domain and the confining walls are embedded in a 2π -periodic square domain (after suitable rescaling), as proposed in [14].

The mask function χ is equal to 0 inside the fluid domain, thus the penalisation terms disappear and the unpenalised MHD equations are recovered. The physical idea is to model the solid part as a porous medium whose permeability ϵ tends to zero [1,16], hence the porous medium tends towards a solid. For $\epsilon \rightarrow 0$, the velocity \mathbf{u} tends to \mathbf{u}_0 and the magnetic field \mathbf{B} tends to \mathbf{B}_0 in the solid domain.

The quantities \mathbf{u}_0 and \mathbf{B}_0 correspond to the values imposed in the solid part of the numerical domain. In previous studies [14,2] we chose $\mathbf{u}_0 = \mathbf{0}$ and $\mathbf{B}_0 = \mathbf{B}_\parallel$, where \mathbf{B}_\parallel is the tangential component of \mathbf{B} at the wall which is not being fixed at a constant value but being re-computed at each time-step. The imposed boundary conditions are thus vanishing velocity and no penetration of magnetic field into the solid domain. The latter is hence considered as a perfect conductor, coated inside with a thin layer of insulant, which guarantees that the current density cannot penetrate into the solid. This type of boundary condition is particularly important when a mean current flows through the domain. In the present work this is not the case and for convenience we assume that $\mathbf{B}_0 = \mathbf{0}$. In tests in two space dimensions it was observed that in the absence of mean currents this choice did not influence the results significantly.

In the case of two-dimensional flow (here in the x - y plane) it is convenient to take the curl of Eqs. (1), (2) to obtain after simplification equations for the vorticity and the current density, which become scalar-valued (in the z -plane) and are perpendicular to the velocity and the magnetic field, respectively.

The vorticity is defined by $\omega \mathbf{e}_z = \nabla \times \mathbf{u}$ and $\mathbf{j} \mathbf{e}_z = \nabla \times \mathbf{B}$ denotes the current density, where \mathbf{e}_z is the unit vector in the z -direction.

$$\frac{\partial \omega}{\partial t} + \mathbf{u} \cdot \nabla \omega = \mathbf{B} \cdot \nabla j + \nu \nabla^2 \omega - \frac{1}{\epsilon} \nabla \times [\chi (\mathbf{u} - \mathbf{u}_0)] \quad (5)$$

$$\frac{\partial j}{\partial t} + \nabla^2 (\mathbf{u} \times \mathbf{B}) = \eta \nabla^2 j - \frac{1}{\epsilon} \nabla \times [\chi (\mathbf{B} - \mathbf{B}_0)] \quad (6)$$

Furthermore we can define the vector potential $\mathbf{a} = a \mathbf{e}_z$ as $\mathbf{B} = \nabla \times \mathbf{a}$ and the stream function ψ as $\mathbf{u} = \nabla^\perp \psi = (-\partial \psi / \partial y, \partial \psi / \partial x)$.

3. Numerical method

3.1. Space discretization

The evolution equations of the vorticity and the current density (5), (6) are transformed into Fourier space in order to compute the spatial derivatives. Hence, the vorticity, the current density and the other variables are represented as truncated Fourier series

$$\omega(\mathbf{x}, t) = \sum_{\mathbf{k} \in \mathbb{Z}^2} \hat{\omega}(\mathbf{k}, t) \exp(i\mathbf{k} \cdot \mathbf{x}) \quad (7)$$

$$j(\mathbf{x}, t) = \sum_{\mathbf{k} \in \mathbb{Z}^2} \hat{j}(\mathbf{k}, t) \exp(i\mathbf{k} \cdot \mathbf{x}) \quad (8)$$

where the Fourier transforms of ω and j are defined as

$$\hat{\omega}(\mathbf{k}, t) = \frac{1}{4\pi^2} \int_{\Omega} \omega(\mathbf{x}, t) \exp(-i\mathbf{k} \cdot \mathbf{x}) d\mathbf{x} \quad (9)$$

$$\hat{j}(\mathbf{k}, t) = \frac{1}{4\pi^2} \int_{\Omega} j(\mathbf{x}, t) \exp(-i\mathbf{k} \cdot \mathbf{x}) d\mathbf{x} \quad (10)$$

with the wavevector $\mathbf{k} = (k_x, k_y)$. The Fourier discretization is uniform in space and is truncated at $k_x = -N_x/2$ and $k_x = N_x/2 + 1$, $k_y = -N_y/2$ and $k_y = N_y/2 + 1$, where N_x and N_y are the number of grid points in x and y direction, respectively.

The derivatives of ω and j are computed by multiplying $\hat{\omega}$ and \hat{j} with $i\mathbf{k}$, respectively, the Laplacian by multiplying with $|\mathbf{k}|^2$. The velocity \mathbf{u} and the magnetic field \mathbf{B} induced by the vorticity ω and the current density j are reconstructed in Fourier space using Biot-Savart's law

$$\mathbf{u}(\mathbf{x}, t) = \sum_{\mathbf{k} \in \mathbb{Z}^2, \mathbf{k} \neq \mathbf{0}} \frac{i\mathbf{k}^\perp}{|\mathbf{k}|^2} \hat{\omega}(\mathbf{k}, t) \exp(i\mathbf{k} \cdot \mathbf{x}) \quad (11)$$

$$\mathbf{B}(\mathbf{x}, t) = \sum_{\mathbf{k} \in \mathbb{Z}^2, \mathbf{k} \neq \mathbf{0}} \frac{i\mathbf{k}^\perp}{|\mathbf{k}|^2} \hat{j}(\mathbf{k}, t) \exp(i\mathbf{k} \cdot \mathbf{x}) \quad (12)$$

where $\mathbf{k}^\perp = (-k_y, k_x)$.

Terms containing products and the penalisation terms, are evaluated by the pseudospectral technique [4] using collocation in physical space. To avoid aliasing errors, i.e. the production of small scales due to the nonlinear terms which are not resolved on the grid, we de-alias at each time step, by truncating the Fourier coefficients of ω (and similarly for j) using the 2/3 rule,

$$\hat{\omega}(\mathbf{k}) = \begin{cases} \hat{\omega}(\mathbf{k}) & \text{for } \left(\frac{3k_x}{2N_x}\right)^2 + \left(\frac{3k_y}{2N_y}\right)^2 < 1 \\ 0 & \text{for } \left(\frac{3k_x}{2N_x}\right)^2 + \left(\frac{3k_y}{2N_y}\right)^2 \geq 1 \end{cases} \quad (13)$$

3.2. Time discretization

For time integration we use a semi-implicit scheme of second order, an Euler–Backward scheme for the linear viscous term and an Adams–Bashforth scheme for the nonlinear terms, see e.g. [16]. The time discretized equations thus read,

$$\sigma \left(\hat{\omega}^{n+1} - \frac{4}{3} \hat{\omega}^n + \frac{1}{3} \hat{\omega}^{n-1} \right) + \nu |\mathbf{k}|^2 \hat{\omega}^{n+1} = \widehat{N_\omega(\omega^*)} \quad (14)$$

$$\sigma \left(\hat{j}^{n+1} - \frac{4}{3} \hat{j}^n + \frac{1}{3} \hat{j}^{n-1} \right) + \eta |\mathbf{k}|^2 \hat{j}^{n+1} = \widehat{N_j(j^*)} \quad (15)$$

where $\sigma = 3/(2\Delta t)$ with Δt the time step, and $\omega^* = 2\omega^n - \omega^{n-1}$ and $j^* = 2j^n - j^{n-1}$. The unknown Fourier coefficients $\hat{\omega}^{n+1}$ and \hat{j}^{n+1} can be obtained by simple division with $\sigma + \nu|\mathbf{k}|^2$ and $\sigma + \eta|\mathbf{k}|^2$, respectively. The explicitly discretized nonlinear terms N_ω and N_j correspond to

$$N_\omega(\omega) = -\mathbf{u} \cdot \nabla \omega + \mathbf{B} \cdot \nabla j - \frac{1}{\epsilon} \nabla \times [\chi(\mathbf{u} - \mathbf{u}_0)] \quad (16)$$

$$N_j(j) = -\nabla^2(\mathbf{u} \times \mathbf{B}) - \frac{1}{\epsilon} \nabla \times [\chi(\mathbf{B} - \mathbf{B}_0)] \quad (17)$$

Due to stability reasons the time step Δt is limited by the penalisation parameter, i.e. $\Delta t < \epsilon$ and the CFL condition $\Delta t < \Delta x/u_{rms}$, with Δx being the spatial grid size and u_{rms} the root mean square velocity.

3.3. Discretisation in three space dimensions

In three space dimensions the numerical scheme is based on the velocity-magnetic field formulation (Eqs. (1), (2)) rather than on the vorticity-current density formulation (Eqs. (5), (6)) as the latter are not scalar-valued quantities anymore.

For spatial discretization we use, as in two space dimensions, a Fourier pseudo-spectral method. For time discretization we use a second order Adams–Bashforth scheme for the nonlinear and penalisation terms, while the linear diffusive term is integrated exactly in time.

The divergence constraint of the velocity is imposed by solving a Poisson equation for the pressure p . To impose the incompressibility of the magnetic field we add a magnetic pressure gradient $\nabla \Pi$ to the induction equation (2) and solve again a Poisson equation for Π . Note that the solution of the Poisson equation becomes trivial in the present case, a simple division by $|\mathbf{k}|^2$ in Fourier space, as periodic boundary conditions are applied in the computational domain Ω .

For periodic boundary conditions (without penalisation terms) the code has been validated by computing the three-dimensional Orszag–Tang vortex, cf. [12].

4. Numerical results

In the following we first present a validation of the code in two space dimensions for the z-pinch configuration, and then we show two-dimensional simulations of decaying MHD turbulence inside an ovoid and in a D-shaped geometry, the latter is motivated by the cross section of a tokamak. Then we also show some preliminary results of three-dimensional decaying MHD turbulence inside a cylinder.

4.1. Z-pinch

In order to check the volume penalisation on the magnetic field, we choose a steady flow problem which has an analytical solution. The z-pinch is a configuration, illustrated in Fig. 1, with a purely

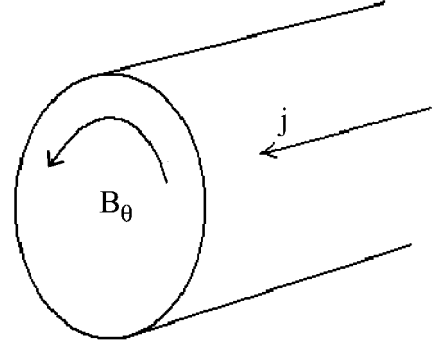


Fig. 1. Configuration of the z-pinch.

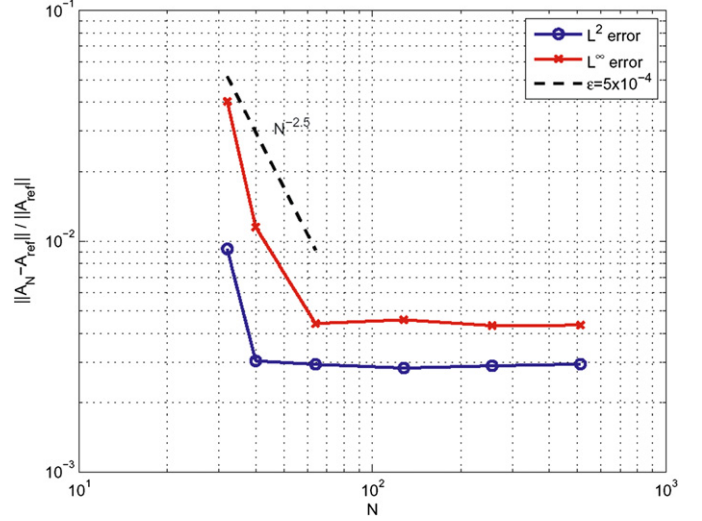


Fig. 2. z-pinch. Decay of the L^2 and L^∞ errors of the vector potential a between the exact and the numerical solution versus the number of grid points.

poloidal magnetic field $\mathbf{B} = (0, B_\theta)$ in plane polar coordinates (r, θ) which consists entirely of the self-induced field by the axial current j [7]. It is well known in the fusion context that the z-pinch represents the radial pressure balance of several interesting fusion concepts, e.g. tokamaks, but its stability properties remain poor if it is not combined with other equilibrium configurations, e.g. the θ -pinch. The analytical steady solution of this problem is given by

$$B^\theta(r) = j_0 r / R \quad (18)$$

$$j(r) = \begin{cases} j_0 & \text{for } |r| < R \\ 0 & \text{for } |r| > R \end{cases} \quad (19)$$

We consider a cylindrical two-dimensional geometry. The computational domain is a periodic square of side length $L_x = L_y = 5$, in which the circle with radius $R = 1$ is imbedded. The fluid domain is thus defined by $\Omega_f = \{\mathbf{x}, |\mathbf{x}|^2 < R\}$ and the solid domain by $\Omega_s = \Omega \setminus \Omega_f$, with $\Omega = [-2.5, 2.5]^2$. The penalisation parameter is $\epsilon = 5 \cdot 10^{-4}$. We impose a constant poloidal value of the magnetic field, $\mathbf{B}_0 = \mathbf{B}_0^\theta = 0.1$, in an annular domain of thickness $\delta = 4\Delta x$ inside the solid domain Ω_s . The viscosity and magnetic diffusivities are $\nu = \eta = 10^{-2}$.

We perform a series of numerical simulations with fixed time step $\Delta t = 4 \cdot 10^{-4}$ varying the spatial resolution, i.e. $N = 32, 40, 64, 128, 256, 512$, until a steady solution has been obtained.

The decay of the L^2 and L^∞ errors of the vector potential a between the exact and the numerical solution as a function of the number of grid points is plotted in Fig. 2. We observe that the errors decay with a slope around -2 which indicates a second order convergence of the scheme for the vector potential. For smaller

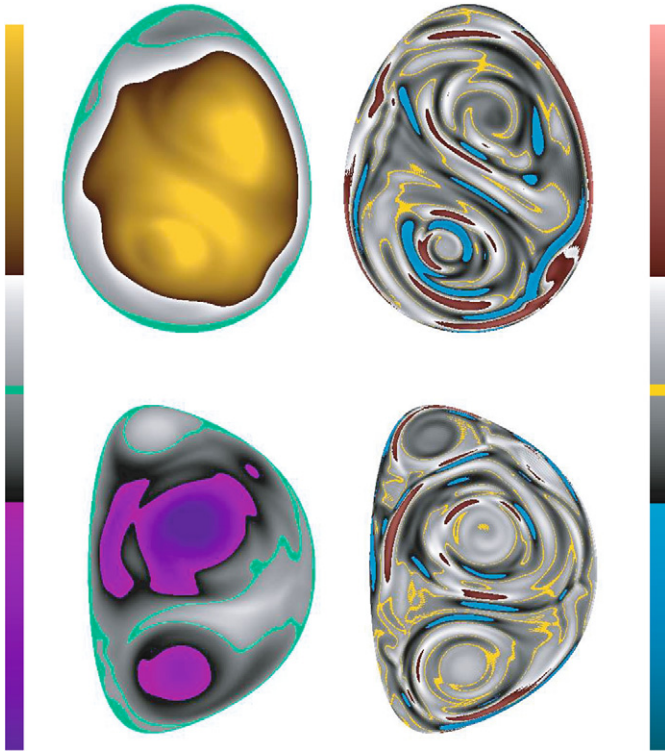


Fig. 3. Two-dimensional magnetized plasma: stream function (left) and vorticity (right). The visualizations correspond to the time-instants at which the absolute value of the angular momentum reaches its maximum.

grid sizes we find a saturation of the errors, which is due to the choice of the penalisation parameter. Smaller values of ϵ will allow for a further decrease of the errors.

4.2. Spontaneous spin-up in non-axisymmetric geometries

Quasi-2D laboratory experiments [11] and two-dimensional numerical simulations of Navier–Stokes flows [5] have revealed the crucial role of the boundaries with no-slip conditions for the velocity on the evolution of the flow inside a container. Indeed, in non-axisymmetric domains (e.g. a square domain [5] or an elliptical domain [9]), boundaries may exert a torque on the fluid and thus increase in short time the kinetic angular momentum of the fluid leading to a spontaneous rotation, called spin-up. This phenomenon implies that a space-filling vorticity structure emerges in the fluid. For a recent review we refer to [6].

In the context of decaying MHD turbulence we have shown that the non-axisymmetry of the domain also produces a spin-up phenomenon [2]. In [2] we considered square and circular domains for relatively low Reynolds numbers. In [3] we studied in addition to square and circular also elliptical domains and showed also that spin-up becomes more pronounced for higher Reynolds numbers.

Here we perform simulations of two-dimensional decaying MHD turbulence inside an ovoid and in a D-shaped geometry starting with random initial conditions. For both geometries we observe that the two-dimensional magnetized plasma self-organizes into a state containing large-scale flow structures, illustrated by the stream function in Fig. 3(left) and vorticity Fig. 3(right).

To quantify the spin-up we consider the angular momentum defined as

$$L_u = \int_{\Omega_f} \mathbf{e}_z \cdot (\mathbf{r} \times \mathbf{u}) ds = 2 \int_{\Omega_f} \psi ds \quad (20)$$

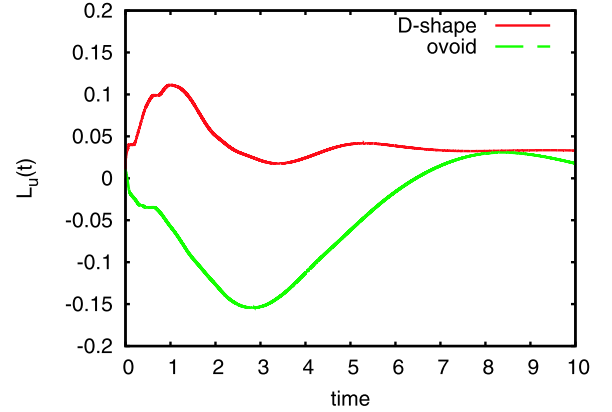


Fig. 4. Time evolution of the angular momentum $L_u(t)$ for the ovoid and the D-shaped geometry.

The surface integral of the vector-product of velocity \mathbf{u} with a vector \mathbf{r} , starting from the center of the flow domain, which is equal to twice the integrated stream function over the fluid domain. L_u quantifies to what amount the fluid is rotating. The maximum angular momentum is obtained for a fluid in solid body rotation. In this particular realization we find that the generation of angular momentum is stronger in the ovoid, than in the D-shaped geometry as shown in Fig. 4.

4.3. Preliminary results in 3D

In this section we present some first, preliminary results of simulations of three-dimensional decaying MHD flows in wall-bounded domains using the volume penalisation method. In the test we present here we impose homogeneous Dirichlet conditions at the wall for both the velocity and the magnetic field, i.e. $\mathbf{u}_0 = 0$ and $\mathbf{B}_0 = 0$.

One simulation is performed in a cylinder using 80^3 Fourier modes. The cylinder is contained in a periodic cubic box of size $L_x = L_y = L_z = 2\pi$. The diameter of the cylinder is equal to 5.8 and the flow is periodic in the z -direction. The diffusivity η and the viscosity ν are equal to 10^{-2} and the permeability parameter, ϵ , is set equal to 10^{-3} . The initial condition consists of divergence-free correlated Gaussian random fields for the velocity and magnetic fields. At the initial state, the kinetic energy is $E_u(0) = \frac{1}{2} \int \mathbf{u}^2 d\mathbf{x} = 1.5$ and the magnetic energy is $E_B(0) = \frac{1}{2} \int \mathbf{B}^2 d\mathbf{x} = 1.6$ leading to an initial Reynolds number around 1100.

Visualizations of vorticity and current density at the time $t = 4$ are presented in Figs. 5 and 6, respectively. We observe regions of coincidence between the maxima of the vorticity and the current density, as observed in the two-dimensional case [14] and regions (see the cross sections in Figs. 5 and 6) with on one hand intense current density and on the other hand vanishing vorticity. In the vicinity of these regions of strong alignment, nonlinear terms will be weak which may thus stabilize the structures. One can also see sheet-like structures of vorticity and current density. In Fig. 7 the time evolution of the L^∞ -norm of the divergence of velocity and of the magnetic field are plotted. We observe that the values remain below 10^{-6} . This confirms that the incompressibility of the numerical scheme for both velocity and magnetic field is satisfied.

5. Conclusions

We presented a Fourier pseudo-spectral method in combination with a volume penalisation approach for the resistive MHD equations in two and three space dimensions. Therewith incompressible electrically conducting flows can be computed efficiently in confined domains of arbitrary shape. Different kinds of boundary

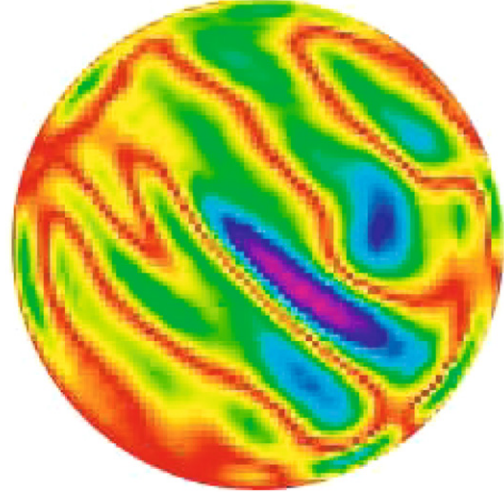
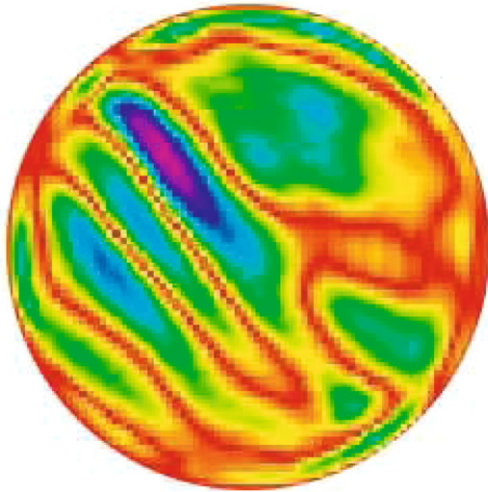
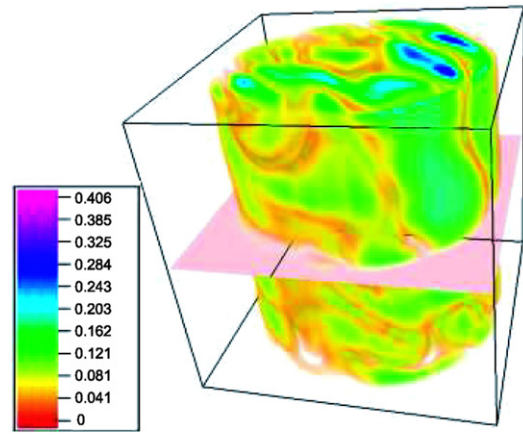
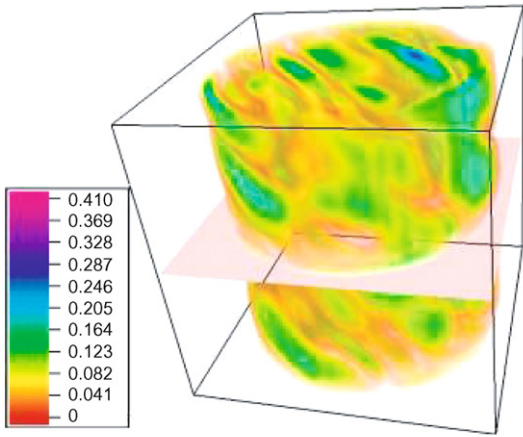


Fig. 5. Decaying MHD turbulence in a cylinder. Volume visualization of modulus of vorticity (top), horizontal cut (bottom).

Fig. 6. Decaying MHD turbulence in a cylinder. Volume visualization of modulus of current density (top), horizontal cut (bottom).

conditions can be imposed while still using a Fourier discretization.

We presented a code validation in two space dimensions for the z-pinch configuration and confirmed previous work by showing that spontaneous spin-up of two-dimensional decaying MHD turbulence takes place in non-axisymmetric geometries. First results of a computation of decaying MHD turbulence in a cylinder are promising and show the potential of the method for three-dimensional simulations.

The pseudospectral method is essentially based on the fast Fourier transforms and thus it can be parallelized efficiently. This will allow to compute three-dimensional MHD turbulence in bounded domains for high Reynolds numbers on massively parallel computers.

Acknowledgements

K.S. thankfully acknowledges financial support from the organizers of the Conference of Computational Physics 2009, held in Kaohsiung, Taiwan and thanks Professor David Montgomery for his kind support.

References

[1] P. Angot, C.H. Bruneau, P. Fabrie, A penalization method to take into account obstacles in viscous flows, *Numer. Math.* 81 (1999) 497.
 [2] W.J.T. Bos, S. Neffaa, K. Schneider, Rapid generation of angular momentum in bounded magnetized plasma, *Phys. Rev. Lett.* 101 (2008) 235003.

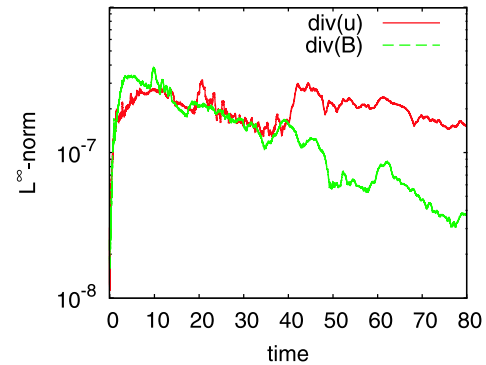


Fig. 7. Decaying MHD turbulence in a cylinder. Evolution of $\|\nabla \cdot \mathbf{u}\|_\infty$ and $\|\nabla \cdot \mathbf{B}\|_\infty$ in log-lin representation.

[3] W.J.T. Bos, S. Neffaa, K. Schneider, Self-organization and symmetry breaking in two-dimensional plasma turbulence, *Phys. Plasmas* 17 (2010), in press.
 [4] C. Canuto, M.Y. Hussaini, A. Quaternioni, T.A. Zang, *Spectral Methods in Fluid Dynamics*, Springer-Verlag, Berlin, Heidelberg, 1988.
 [5] H.J.H. Clercx, S.R. Maassen, G.J.F. van Heijst, Spontaneous spin-up during the decay of 2D turbulence in a square container with rigid boundaries, *Phys. Rev. Lett.* 80 (1998) 5129.
 [6] H.J.H. Clercx, G.J.F. van Heijst, Two-dimensional Navier-Stokes turbulence in bounded domains, *Appl. Mech. Rev.* 62 (2009).
 [7] J.P. Freidberg, *Ideal magnetohydrodynamic theory of magnetic fusion systems*, *Rev. Modern Phys.* 54 (3) (1982) 801.
 [8] T. Ishihara, T. Gotoh, Y. Kaneda, Study of high Reynolds number isotropic turbulence by direct numerical simulation, *Annu. Rev. Fluid Mech.* 41 (2009) 65.

- [9] G.H. Keetels, H.J.H. Clercx, G.J.F. van Heijst, Spontaneous angular momentum generation of 2D flows in an elliptical geometry, *Phys. Rev. E* 78 (2008) 036301.
- [10] D. Kolomenskiy, K. Schneider, A Fourier spectral method for the Navier–Stokes equations with volume penalization for moving solid obstacles, *J. Comput. Phys.* 228 (2009) 5687.
- [11] S.R. Maassen, H.J.H. Clercx, G.J.F. van Heijst, Decaying quasi-2D turbulence in a stratified fluid with circular boundaries, *Europhys. Lett.* 46 (3) (1999) 339–345.
- [12] P.D. Mininni, A.G. Pouquet, D.C. Montgomery, Small scale structures in three-dimensional magnetohydrodynamic turbulence, *Phys. Rev. Lett.* 97 (2006) 244503.
- [13] P.D. Mininni, D.C. Montgomery, Magnetohydrodynamic activity inside a sphere, *Phys. Fluids* 18 (2006) 116602.
- [14] S. Neffaa, W.J.T. Bos, K. Schneider, The decay of magnetohydrodynamic turbulence in a confined domain, *Phys. Plasmas* 15 (2008) 092304.
- [15] K. Reuter, F. Jenko, C.B. Forest, R.A. Bayliss, A parallel implementation of an MHD code for the simulation of mechanically driven, turbulent dynamos in spherical geometry, *Comput. Phys. Comm.* 179 (4) (2008) 245–249.
- [16] K. Schneider, Numerical simulation of the transient flow behaviour in chemical reactors using a penalization method, *Comput. & Fluids* 34 (2005) 1223.
- [17] K. Schneider, M. Farge, Decaying two-dimensional turbulence in a circular container, *Phys. Rev. Lett.* 95 (2005) 244502.